



Article

Adsorption of Anionic and Cationic Dyes on Activated Carbon Prepared from Oak Cupules: Kinetics and Thermodynamics Studies

Manal Alkhabbas * , Alaa M. Al-Ma'abreh * , Gada Edris, Tasneem Saleh and Heba Alhmoody

Department of Chemistry, Faculty of Science, Isra University, Amman 11622, Jordan

* Correspondence: manal.khabbas@iu.edu.jo (M.A.); alaa.almaabreh@iu.edu.jo (A.M.A.-M.);

Tel.: +96-2796865552 (M.A.); +96-2799011634 (A.M.A.-M.)

Abstract: In this study, activated carbon produced from oak cupules (ACOC) was prepared using chemical activation with H_3PO_4 . ACOC is subsequently used as an adsorbent to facilitate the removal of an acidic dye, naphthol blue black (NBB), and basic dye crystal violet (CV) from aqueous solutions. The ACOC was characterized by FTIR spectroscopy, XRD, and SEM. The adsorption isotherm data fits well with the Langmuir model for NBB and CV. The kinetic models of adsorption of NBB and CV by ACOC were pseudo-first order and pseudo-second order, respectively. Thermodynamic parameters were evaluated and indicated that the adsorption of both dyes onto ACOC was endothermic and spontaneous. The adsorption capacity of ACOC reached 208 mg g^{-1} for NBB and 658 mg g^{-1} for CV. ACOC was shown to be a promising adsorbent for the removal of NBB and CV from aqueous solutions.

Keywords: wastewater treatment; adsorption; activated charcoal; oak cupules; naphthol blue black; crystal violet



Citation: Alkhabbas, M.;

Al-Ma'abreh, A.M.; Edris, G.; Saleh, T.; Alhmoody, H. Adsorption of Anionic and Cationic Dyes on Activated Carbon Prepared from Oak Cupules: Kinetics and Thermodynamics Studies. *Int. J. Environ. Res. Public Health* **2023**, *20*, 3280. <https://doi.org/10.3390/ijerph20043280>

Academic Editor: Paul B.

Tchounwou

Received: 3 January 2023

Revised: 8 February 2023

Accepted: 10 February 2023

Published: 13 February 2023



Copyright: © 2023 by the authors. Licensee MDPI, Basel, Switzerland. This article is an open access article distributed under the terms and conditions of the Creative Commons Attribution (CC BY) license (<https://creativecommons.org/licenses/by/4.0/>).

1. Introduction

The textile, pulp, and paper industries produce various contaminants, such as dyes and pigments, which are discharged as wastewater. Due to their chemical structure, the dyes are characterized by thermal stability and photostability, and they are also resistant to biodegradation. As a result, they last in the environment for a long time. Dyes absorb and reflect the sunlight that penetrates water, which affects the photosynthesis process of algae and therefore the food chain. Several dyes have been found to be carcinogenic, mutagenic, teratogenic, and toxic to living creatures. Thus, their removal from wastewater is a necessity [1,2].

Naphthol blue black (NBB) dye (Figure 1a) belongs to the azo group dyes that contain one azo group ($-N=N-$) at least [3]. NBB dye is classified as an anionic or acidic dye due to the existence of a sulfonate group ($-SO_3^-$). Crystal violet (CV) dye (Figure 1b) is a member of the triphenylmethane dyes, and it is classified as a cationic or basic dye [4].

Several chemical, physical, and biological techniques are suggested for the removal of organic pollutants from wastewater including adsorption, flocculation–coagulation, sedimentation, dialysis, chemical oxidation, ion exchange, membrane separation and biodegradation [5,6]. Adsorption is one of the most effective techniques that is employed for the removal of pollutants from wastewater because it is inexpensive, efficient, simple, and easy to manage [7].

In adsorption, the most widely applied adsorbent is activated charcoal (AC), which is a carbonaceous material produced from wood, coconut shells, soy meal hull, etc. AC is characterized by high porosity and high adsorption capacity. Additionally, it is employed as an adsorbent for the removal of several organic pollutants from air and water. AC was

prepared from several types of agricultural waste and was employed for the elimination of different dyes from aqueous solutions [8,9].

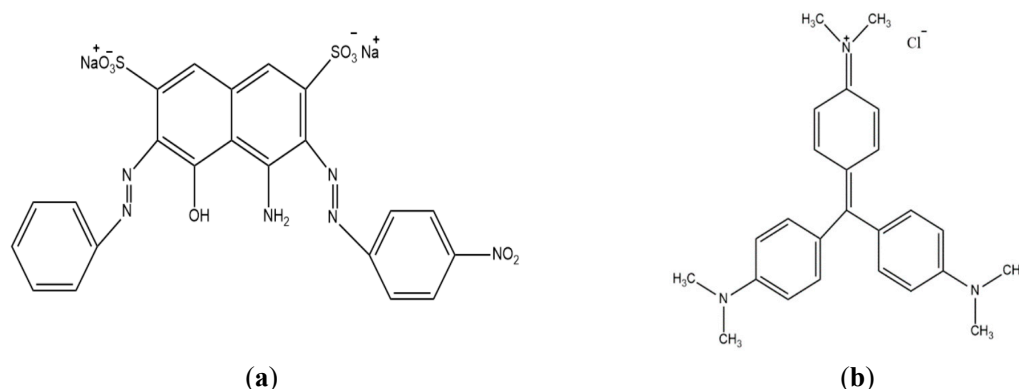


Figure 1. Structure of (a) naphthol blue black and (b) crystal violet.

The aim of this study is to prepare activated charcoal from oak cupules (cost-free forestry waste) by chemical activation using phosphoric acid. Activated carbon prepared using oak cupules (ACOC) is used to investigate the adsorption capacity for anionic and cationic dyes' removal, namely NBB and CV, from aqueous solutions. The effects of several factors, such as contact time, adsorbent dose, dye concentration, pH and temperature, are closely examined. The properties of the prepared activated charcoal are analyzed using Fourier transform infrared (FTIR), scanning electron microscopy (SEM), and X-ray diffraction (XRD).

2. Experimental

2.1. Preparation of the Adsorbate Solutions

The anionic dye (NBB) and cationic dye (CV) were purchased from Sigma-Aldrich. The chemical structures of NBB and CV are shown in Figure 1. The NBB and CV stock solutions of 1.0 g L^{-1} concentration were prepared, and the desired experimental concentrations were made up by diluting the stock solution with distilled water. The pH of solutions was adjusted using 0.1 M HCl and 0.1 M NaOH solutions.

2.2. Preparation of the Activated Charcoal

The oak cupules (OC) were gathered from Jerash Province in Jordan, washed with distilled water to get rid of any adhering impurities, and then dried in an air oven at $100 \text{ }^\circ\text{C}$ for 24 h. This was followed by grinding and sieving to obtain particle sizes less than 0.5 mm. H_3PO_4 (85%) was added to oak cupules in a ratio of 3:1 (g H_3PO_4 /g oak cupules). The resulting slurry was then left overnight, then dried at $120 \text{ }^\circ\text{C}$ for 4 h. Afterwards, the mixture was heated in a muffle furnace at $450 \text{ }^\circ\text{C}$ for 1 h. The activated carbon was washed with warm distilled water and a 1.0 M NaOH solution until pH 7, then washed with distilled water. Finally, the prepared ACOC was dried at $110 \text{ }^\circ\text{C}$ for 6 h.

2.3. Characterizations of the Activated Charcoal

The prepared ACOC adsorbent was characterized before and after the adsorption. Scanning electron microscopy (SEM) (FEI Company; Inspect F50 High Vacuum 6×10^{-4} Pa, Eindhoven, NB, USA) was used to analyze the surface morphology of the samples. Functional groups of the adsorbent's surface were determined by FTIR (FTIR-7600 Fourier Transform Infrared Spectrometer, lambda USA) in the wavelength range of $450\text{--}4000 \text{ cm}^{-1}$. The structural properties of the samples were analyzed using powdered x-ray diffraction (XRD-7000 X-Ray Diffractometer from Shimadzu, Japan) with a nickel-filtered copper radiation ($\text{CuK}\alpha$) and $\lambda = 1.5456 \text{ \AA}$; the 2θ range scan was performed from 2° to 60° with a step size of 0.02° .

The pH of the point of zero charge (pH_{PZC}) of ACOC was measured by adding 0.05 g of ACOC to a solution of $10^{-2} \text{ mol L}^{-1}$ of KNO_3 with an initial pH of 2–12; the initial pH of the KNO_3 solution was adjusted using HCl and NaOH solutions. The mixture was stirred for 24 h in a shaker until equilibrium at 25°C . The final pH values of the solutions were recorded [10,11].

2.4. Batch Adsorption Experiments

Adsorption studies of NBB and CV dyes were performed using ACOC as the adsorbent. The batch experiments were conducted using a known quantity of adsorbent and a volume of 100 mL of dye solution at a known initial concentration in an Erlenmeyer flask. The flask was placed in a shaker at 120 rpm and a temperature of 25°C . The samples were examined at certain time intervals, and the solutions were filtered using a $0.25\text{-}\mu\text{m}$ syringe filter. The concentration of samples was analyzed using UV-visible double-beam spectrophotometer (UV-6100 PC, China) at $\lambda_{\text{max}} = 618$ and 583 nm for NBB and CV, respectively. The effect of adsorbent dose, reaction time, initial dye concentration, pH and temperature were evaluated. The adsorption capacity, q_e (mg g^{-1}), and the adsorption efficiency, R (percent of adsorbate adsorbed), were calculated using Equations (1) and (2):

$$q_e = \frac{(C_i - C_e)}{m_{\text{ACOC}}} \times V \quad (1)$$

$$R = \frac{(C_i - C_e)}{C_i} \times 100\% \quad (2)$$

where C_i and C_e are the initial concentration and equilibrium concentration of the NBB and CV solutions (mg L^{-1}), respectively, m_{ACOC} is the mass of adsorbent (g), and V (L) is the volume of the solution.

The amount of dye adsorbed at any time, q_t (mg g^{-1}), was calculated by Equation (3):

$$q_t = \frac{(C_i - C_t)}{m_{\text{ACOC}}} \times V \quad (3)$$

where C_t (mg L^{-1}) is the dye concentration at time t .

2.5. Isotherm and Kinetic Studies

Analyzing the adsorption isotherm data is important to investigate the interaction between the adsorbent and the adsorbate, and it is necessary to understand the adsorption mechanisms. Three isotherm models (Langmuir, Freundlich, and Temkin) were used to study the behavior of NBB and CV adsorption on the ACOC. The parameters and equations for the selected isotherm models are listed in Table 1. The kinetics of adsorption are employed to investigate the adsorption dynamics. The parameters and equations for the selected kinetic models are shown in Table 1 [12].

2.6. Adsorption Thermodynamic

The thermodynamic parameters (Gibbs free energy (ΔG°), enthalpy (ΔH°), and entropy (ΔS°)) are given by the following equations:

$$\Delta G^\circ = -RT \ln(K_d) \quad (4)$$

$$\Delta G^\circ = \Delta H^\circ - T\Delta S^\circ \quad (5)$$

where R is the universal gas constant ($8.314 \text{ J}\cdot\text{mol}^{-1}\cdot\text{K}^{-1}$), T is absolute temperature in Kelvin (K) and K_d is the apparent adsorption equilibrium constant, and can be determined as follows:

$$K_d = \frac{q_e}{C_e} \quad (6)$$

ΔH° and ΔS° were computed from adsorption data at different temperatures using the Van't Hoff Equation:

$$\ln(K_d) = \frac{1}{R} \left(\Delta S^\circ - \frac{\Delta H^\circ}{T} \right) \tag{7}$$

Table 1. Equations and parameters of isotherm and kinetics models.

Model	Name	Nonlinear Equation	Linear Equation	Parameters
Isotherm	Langmuir	$q_e = \frac{q_m k_l C_e}{1 + k_l C_e}$	$\frac{C_e}{q_e} = \frac{1}{k_l q_m} + \frac{C_e}{q_m}$	C_e : Concentration of dye at equilibrium (mg L^{-1}) q_e : Amount of adsorbate adsorbed per unit mass of adsorbent at equilibrium (mg g^{-1}) q_m : Theoretical maximum adsorption capacity (mg g^{-1}) k_l : Langmuir constant related to the rate of adsorption $1/n$ and K_F : Freundlich constants k_t : Temkin constant
	Freundlich	$q_e = K_f C_e^{1/n}$	$\ln q_e = \ln K_f + \frac{1}{n} \ln C_e$	
	Temkin	$q_e = q_m \ln(k_T C_e)$	$q_e = q_m \ln k_T + q_m \ln C_e$	
Kinetics	Pseudo-first order	$q_t = q_e (1 - \exp^{-k_{1p} t})$	$\ln(q_e - q_t) = \ln q_e - k_{1p} t$	q_t : Amount of adsorbate adsorbed per unit mass of adsorbent at time t constant (mg g^{-1}) k_{1p} : Pseudo-first order rate constant k_2 : Second order rate constant k_{2p} : Second order rate constant k_{int} : Intraparticle diffusion rate constant
	Second order	$q_t = \frac{q_e}{(1 + k_2 q_e t)}$	$\frac{1}{q_t} = \frac{1}{q_e} + k_2 t$	
	Pseudo-second order	$q_t = \frac{k_{2p} q_e^2 t}{1 + k_{2p} q_e t}$	$\frac{t}{q_t} = \frac{1}{k_{2p} q_e} + \frac{t}{q_e}$	
	Intraparticle diffusion	$q_t = k_{int} t^{1/2}$		

3. Results and Discussion

3.1. Characterization of Adsorbate

The FTIR spectra of ACOC in the range ($4000\text{--}500\text{ cm}^{-1}$) before and after the adsorption is provided in Figure 2. The peak at about 3425 cm^{-1} might be attributed to the hydroxyl groups (--OH) of adsorbed water or phenolic group at the ACOC, and this peak is shifted to 3389 cm^{-1} and 3396 cm^{-1} due to the adsorption of NBB and CV, respectively. The shift that occurred might be attributed to the hydrogen bonding that forms between the hydroxyl group on ACOC and the functional groups on the dyes. The peak at 1630 cm^{-1} is attributed to the carbonyl group at ACOC, and it appeared as a broad band and shifted to a lower frequency after adsorption of NBB and CV, respectively. The band at about 1560 cm^{-1} might be attributed to aromatic C=C stretching [13].

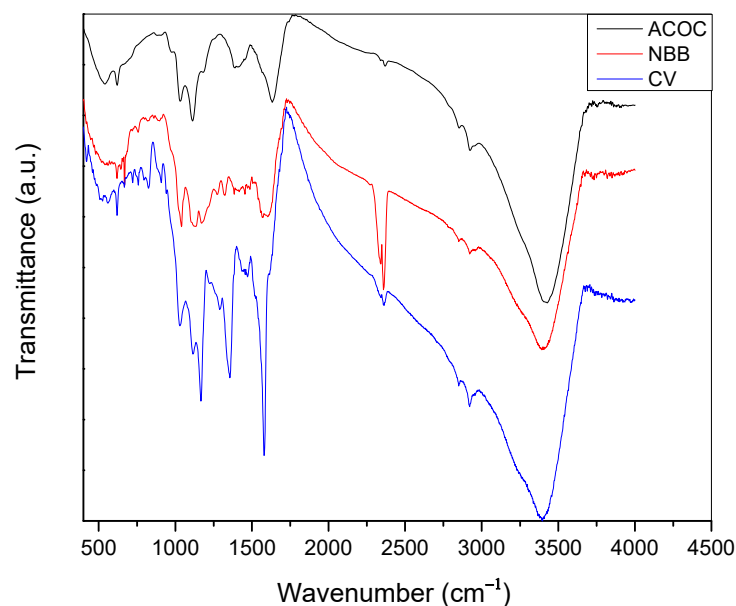


Figure 2. IR spectra of ACOC, ACOC after adsorption of NBB and ACOC after adsorption of CV.

SEM analysis was employed to study the surface morphology of ACOC before and after the adsorption of NBB and CV. Figure 3a shows the SEM image of ACOC; several pores with varied sizes were observed on the surface of the ACOC. Figure 3b,c display the aggregation of NBB and CV, respectively, on the surface of ACOC.

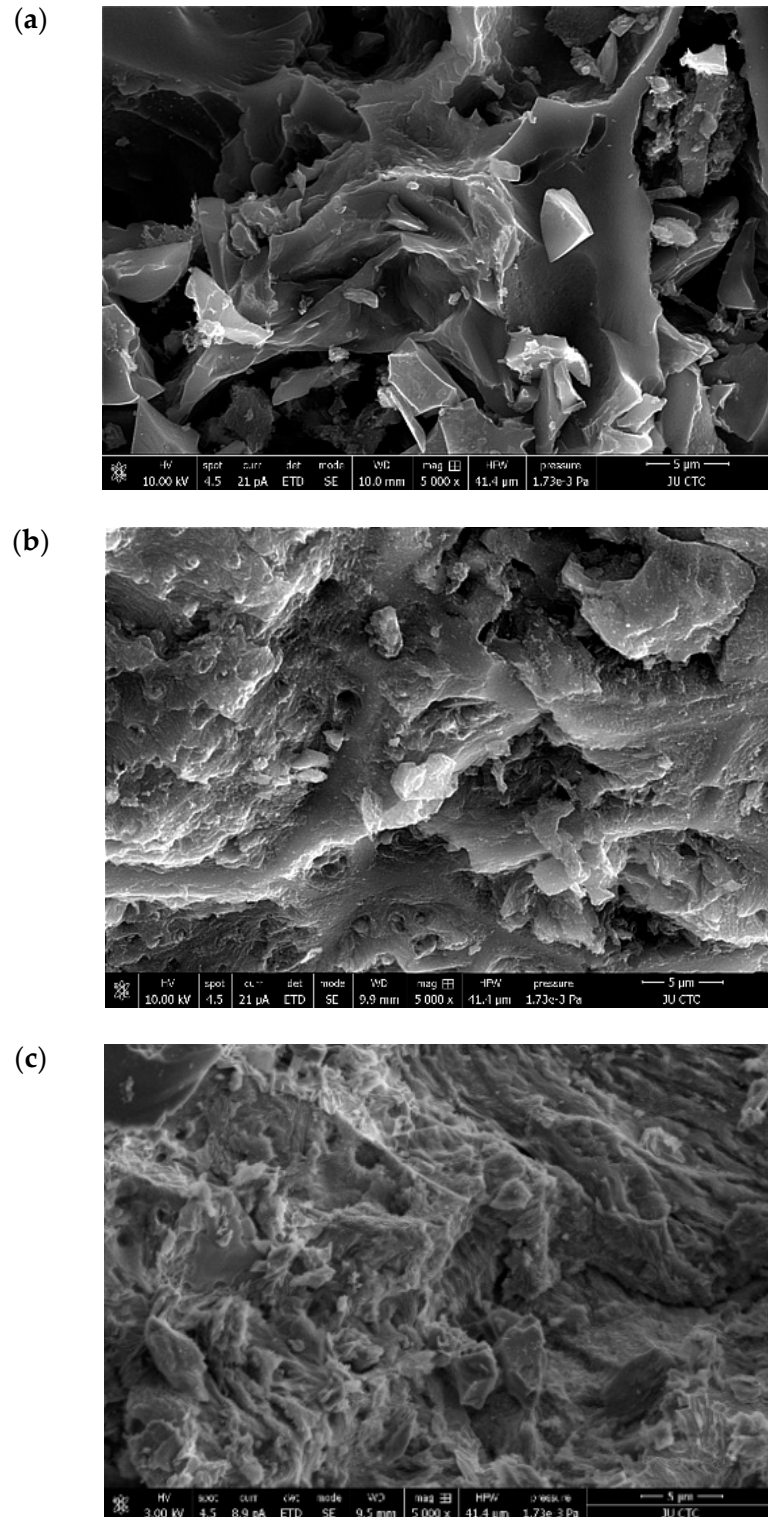


Figure 3. SEM images of ACOC (a) before adsorption (b) after adsorption of NBB and (c) after adsorption of CV.

The XRD patterns of ACOC before and after adsorption of dyes are shown in Figure 4. The broadening in the peaks of the XRD diffractograms is an indication of the amorphous nature of the activated carbon. The position of the peak for ACOC (before and after adsorption) is observed at about 24° , and the result is identical to that obtained in previous studies [14]. An increase in the intensity of XRD peaks is observed after the adsorption of both dyes.

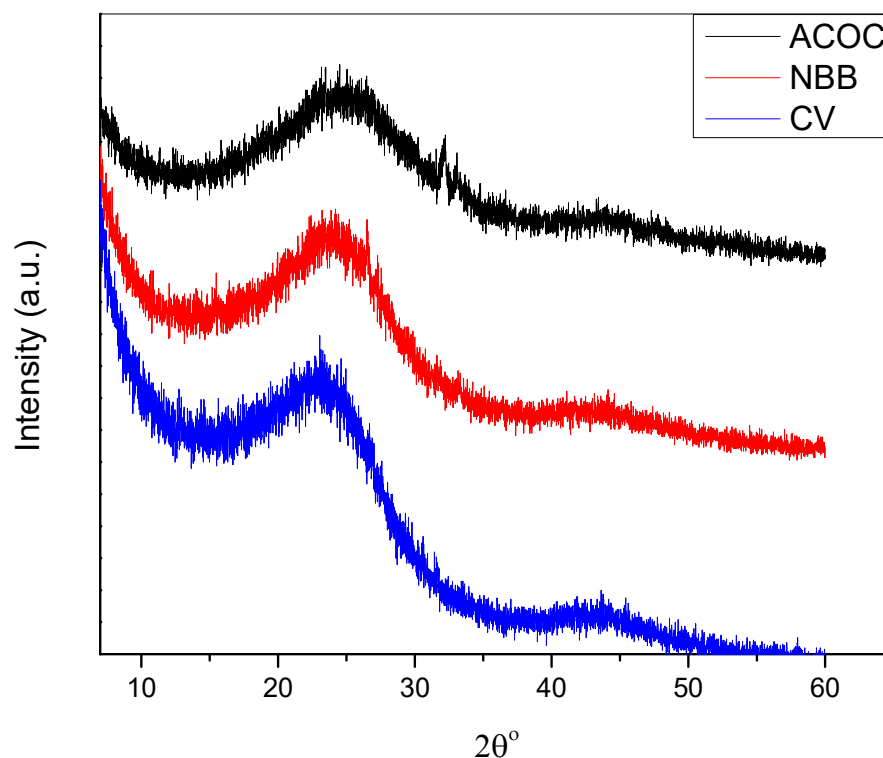


Figure 4. XRD spectra of ACOC before adsorption and after adsorption of NBB and CV.

The charge and functional groups on the adsorbent surface are affected by the pH of the solution. The pH_{pzc} of ACOC was observed to be 6.96 (Figure 5). At pH_{pzc} , the surface charge of ACOC is zero. As a result, the electrostatic interactions between the positive and negative charges of ACOC are equal [10]. Additionally, it can be observed that the final pH of the solution approaches the initial pH of the solution at $\text{pH} = 2$ and $\text{pH} = 12$; this can be attributed to the high concentration of hydronium ions at $\text{pH} = 2$ and the high concentration of hydroxide ions at $\text{pH} = 12$. So, relatively, a small fraction of hydronium ions and hydroxide ions will be attracted to the negative and positive charges, respectively, on the surface. Thus, a subtle change of pH will occur at high and low values of pH.

3.2. Parametric Study of the Adsorption Process

3.2.1. Effect of Contact Time

The contact time was investigated up to 240 min, as displayed in Figure 6, with a dye concentration of 100 mg L^{-1} , a temperature of 25°C , and an ACOC dose of 0.3 g L^{-1} . The adsorption of both dyes is increased with increasing time until it reaches equilibrium after 180 min for NBB, with 60% removal, and 90 min for CV, with 98% removal.

3.2.2. Effect of ACOC Dose

The ACOC dose was investigated in the range of 0.02–0.08 g for NBB and of 0.01–0.04 g for CV. The dye concentration was 100 mg L^{-1} and the volume of solution was 100 mL. Figure 7 shows the percentage of removal and the adsorption capacity of ACOC (mg dye/g ACOC). The removal percentage was increased from 42% to 98% and from 66% to 98% for NBB and CV, respectively. It is obvious that when the adsorbent dose increases, the removal

percentage of the dye increases. This is attributed to the increase in the number of available sites for the adsorption. The adsorption capacity of ACOC reached 208 mg g^{-1} for NBB and 658 mg g^{-1} for CV. The adsorption capacity decreases as the amount of ACOC increases, and this is due to the unsaturation of available sites [15]. The adsorption capacity at 0.02 g of ACOC was 208 mg g^{-1} ($0.337 \text{ mmol g}^{-1}$) for NBB and 418 mg g^{-1} ($1.025 \text{ mmol g}^{-1}$) for CV, respectively; thus, the adsorption capacity of particles at the ACOC surface for CV is about three times larger than that for NBB.

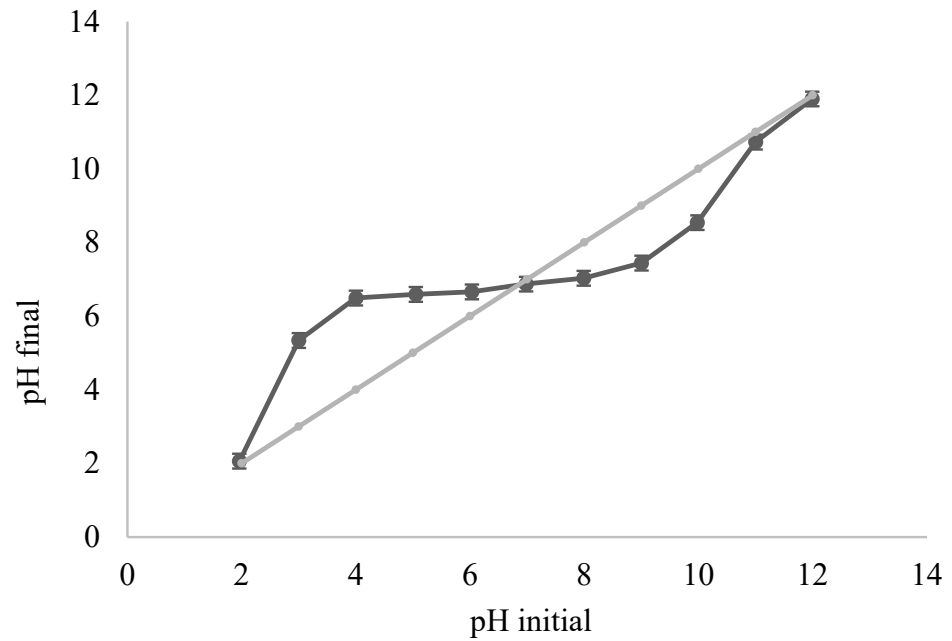


Figure 5. pH_{pzc} determination of ACOC.

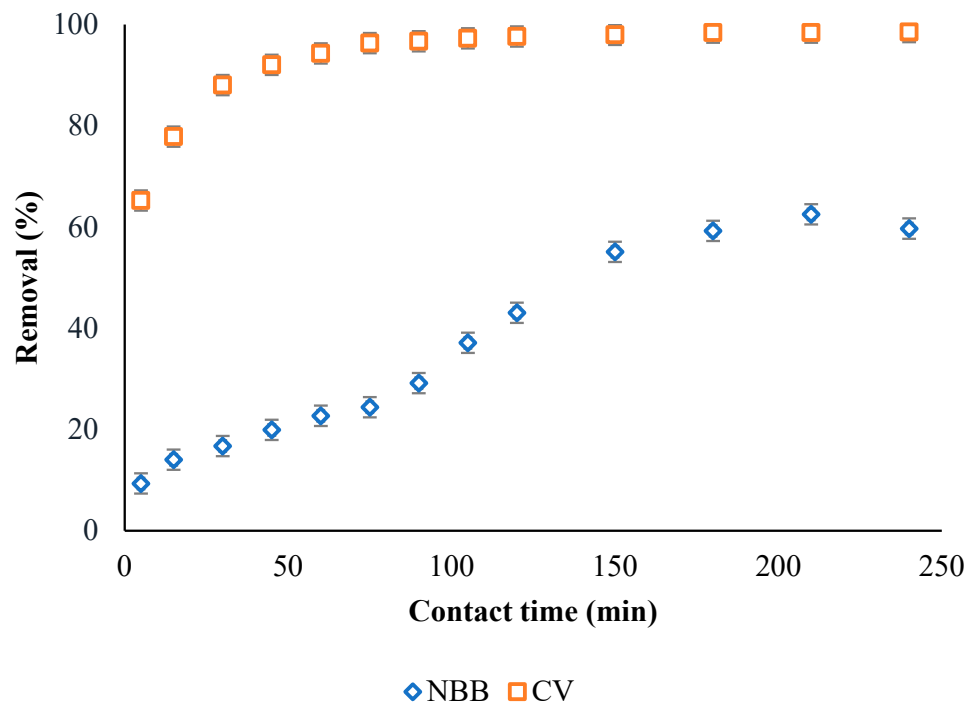


Figure 6. Effect of contact time on the removal of 100 mg L^{-1} initial dye concentration of NBB and CV by 0.3 g L^{-1} of ACOC.

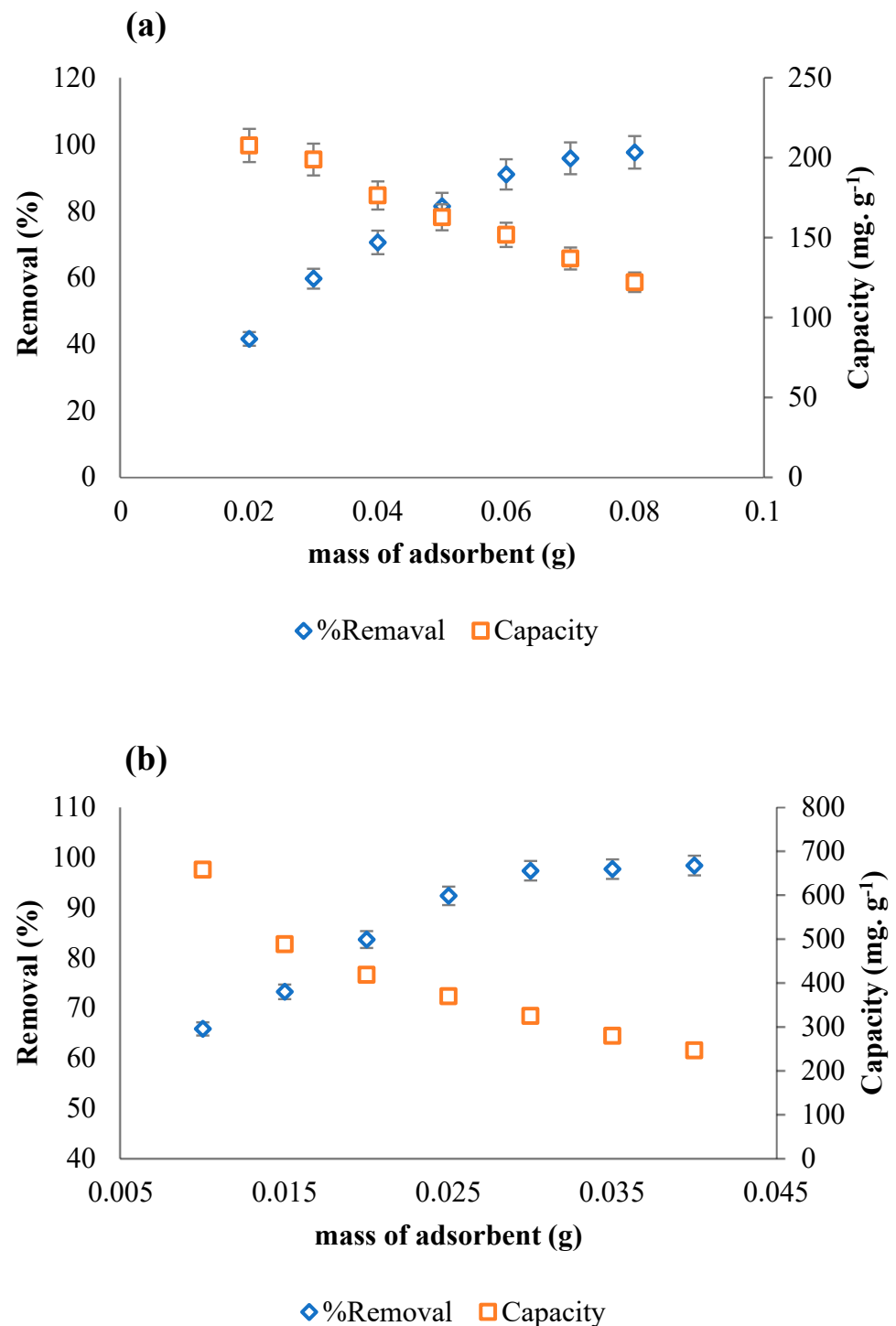


Figure 7. Effect of the ACOC dose on the removal of 100 mg L^{-1} (a) NBB and (b) CV (T: $25 \text{ }^{\circ}\text{C}$, V = 100 mL).

3.2.3. Effect of Dye Concentration

The effect of initial dye concentrations was examined in the range of $50\text{--}175 \text{ mg L}^{-1}$ for NBB ($m_{\text{ACOC}} = 0.05 \text{ g}$) and $50\text{--}130 \text{ mg L}^{-1}$ for CV ($m_{\text{ACOC}} = 0.02 \text{ g}$). As Figure 8 shows, the removal efficiency of both dyes is decreased as the initial concentration of the dyes increases, and this may be attributed to the limited number of adsorption sites that are present on the ACOC surface [7].

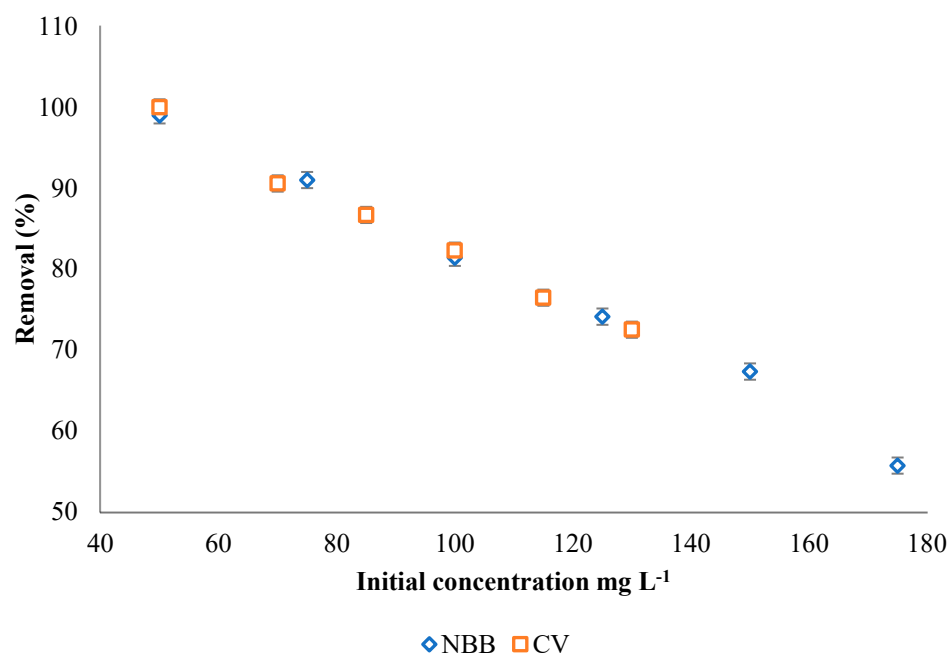


Figure 8. Effect of initial dye concentration of NBB and CV on the adsorption efficiency of ACOC ($T = 25\text{ }^{\circ}\text{C}$, $V = 100\text{ mL}$, m_{ACOC} is 0.050 g for NBB and 0.020 g for CV; contact time is 210 min. for NBB and 120 min. for CV).

3.2.4. Effect of pH

The effect of the pH on removal efficiency was investigated at various pH values as shown in Figure 9. For NBB dye, the removal efficiency decreases as pH increases, while for CV dye, the removal efficiency increases as pH increases. At $\text{pH} < \text{pH}_{\text{PZC}}$, the surface of the ACOC has a positive charge and will attract the negative anionic NBB dye species, and at $\text{pH} > \text{pH}_{\text{PZC}}$, the surface of the ACOC has a negative charge and will attract the positive cationic CV dye species. According to previous studies, the removal efficiency for cationic dyes is enhanced when the pH is higher than the pH_{PZC} [12], and the removal efficiency for anionic dyes is enhanced when pH is lower than the pH_{PZC} [16].

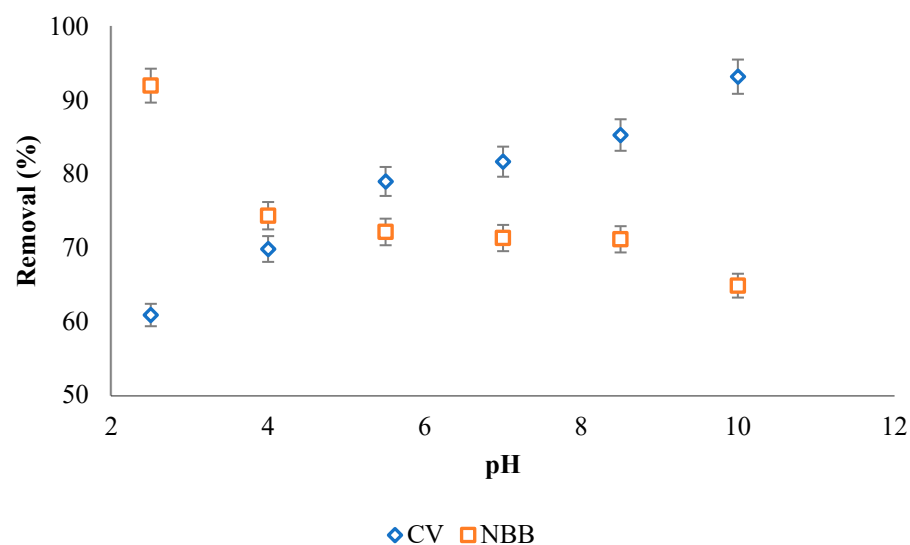


Figure 9. The effect of pH on 100 mg g^{-1} NBB and CV removal efficiency by ACOC ($T = 25\text{ }^{\circ}\text{C}$, $V = 100\text{ mL}$, m_{ACOC} is 0.050 g for NBB and 0.020 g for CV).

3.2.5. Effect of Temperature

The effect of adsorption temperature is examined at a temperature of 30, 35 and 40 °C for 100 mg L⁻¹ of the NBB and CV dyes, as shown in Figure 10. The removal efficiency of both dyes increases as the adsorption temperature increases. The results indicate the endothermic nature of the adsorption reaction for both dyes onto ACOC surface.

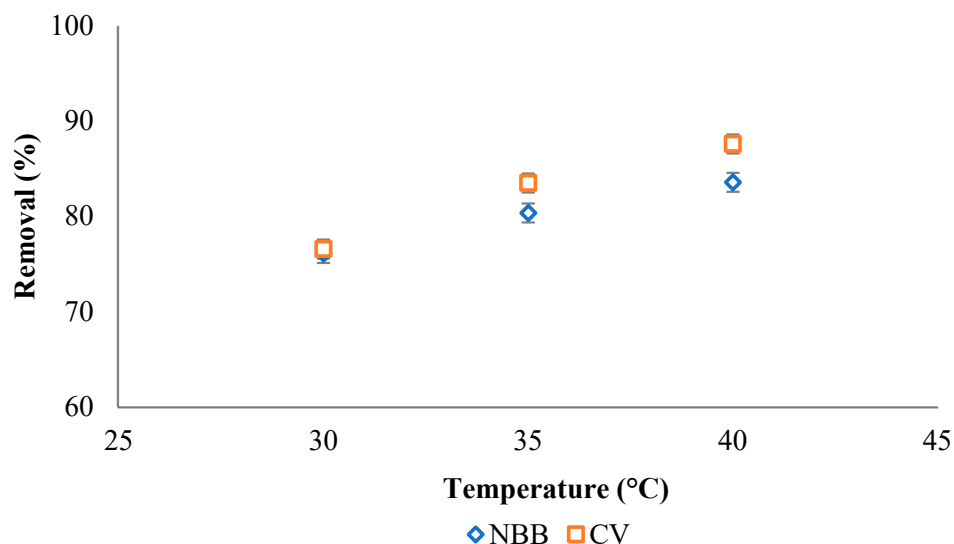


Figure 10. Effect of temperature on the efficiency of removal of 100 mg L⁻¹ NBB and CV dyes onto ACOC.

3.3. Isotherm Studies

The mechanism of adsorption for NBB and CV dyes onto ACOC was investigated by Langmuir, Freundlich, and Temkin isotherm models. Table 2 summarizes the achieved results, including correlation coefficients and constants. The Langmuir model introduces the best fit for both dyes, with maximum R^2 for NBB ($R^2 = 0.992$) and CV ($R^2 = 0.935$). In the Langmuir model, the q_m value was found to be 213 and 625 mg g⁻¹ for NBB and CV, respectively, and these values agree with the experimental ones. Additionally, the k_L value of NBB (0.2814) was larger than that of CV (0.2462), demonstrating that ACOC has greater adsorption energy with NBB than CV [13]. The Langmuir model fit indicates the formation of a monolayer of dye adsorbed at ACOC, with little interaction between the adsorbed species. In the Freundlich model, the values of $1/n$ were 0.1585 for NBB and 0.2572 for CV; this suggested favorable adsorption of both dyes ($0.1 < \frac{1}{n} < 1$) at ACOC [15]. The smallest values for R^2 for both dyes were calculated using the Temkin model. q_m values were 25.5 and 103.5 for NBB and CV, respectively, and these values are far from the experimental values for both dyes. Equilibrium plots of the three isotherm models and the experimental data for the adsorption of NBB and CV onto ACOC are shown in Figure 11.

Table 2. Isotherm models parameters for the adsorption of NBB and CV dyes on ACOC.

Model	Parameter	NBB	CV
Langmuir	q_m (mg g ⁻¹)	213	625
	k_L	0.2814	0.2462
	R^2	0.992	0.935
	$1/n$	0.1585	0.2572
Freundlich	K_f	106.9	227
	R^2	0.9768	0.9164
Temkin	q_m (mg g ⁻¹)	25.5	103.5
	k_T	46.0	6.41
	R^2	0.9570	0.8475

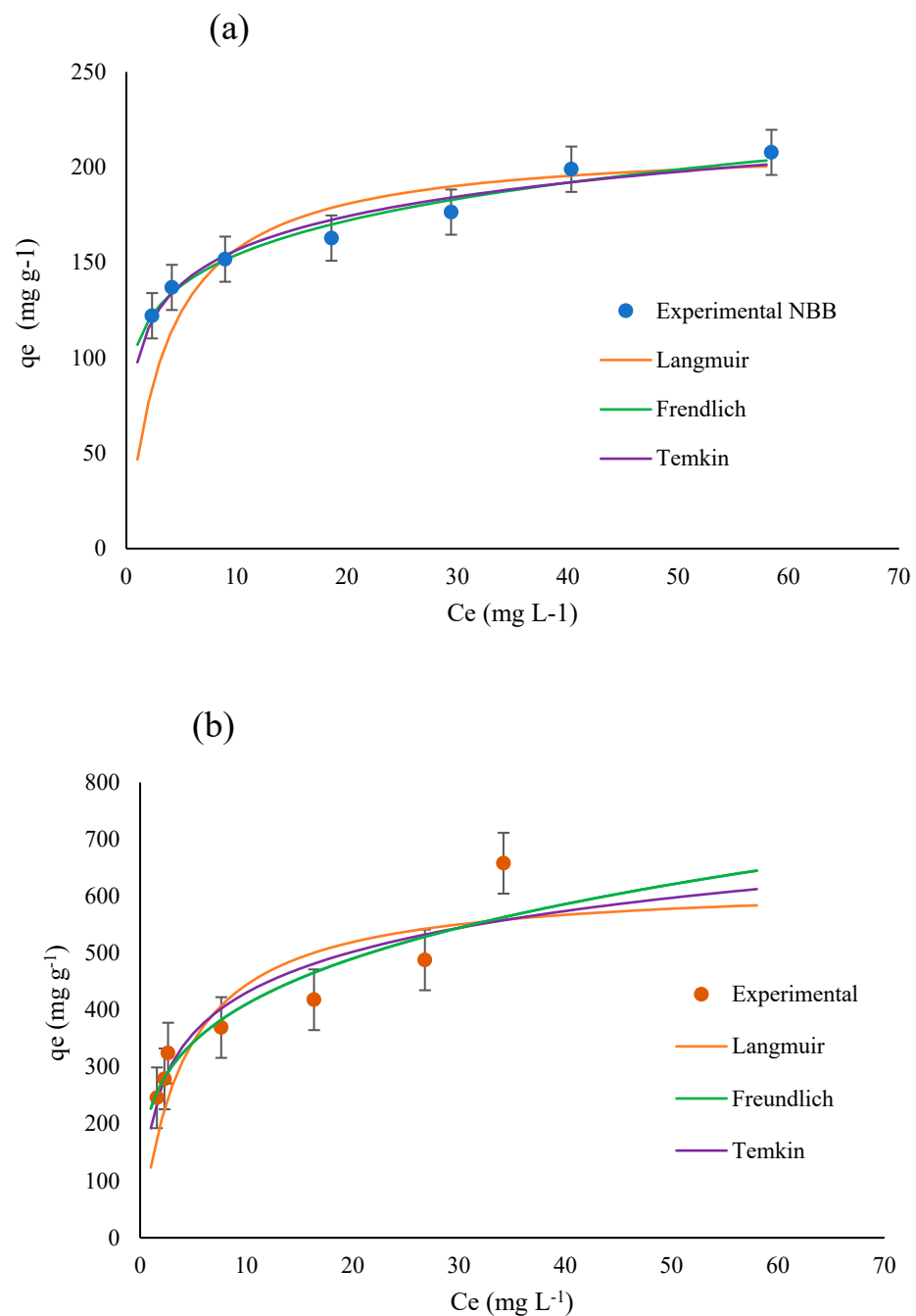


Figure 11. Adsorption isotherm models (Langmuir, Freundlich and Temkin) fitted to experimental adsorption of (a) NBB and (b) CV.

3.4. Kinetics Study

Pseudo-first order, second order, pseudo-second order, and intraparticle diffusion kinetic models were used in this study. The obtained parameters for these models are listed in Table 3. Based on the highest correlation coefficient values, the adsorption of NBB follows the pseudo-first order kinetic model ($R^2 = 0.9917$), and the adsorption of CV follows the pseudo-second order kinetic model ($R^2 = 0.9917$). Due to the nonzero intercept, the interparticle diffusion model did not fit with the experimental data for both dyes.

Table 3. Kinetics models parameters for the adsorption of NBB and CV dyes on ACOC.

Model	Parameter	NBB	CV
Pseudo-first order	K_{1p}	0.0173	0.0202
	q_e	125	66.3
	R^2	0.9917	$R^2 = 0.9439$
Second order	k_2	$-(4 \times 10^{-5})$	$-(2 \times 10^{-6})$
	q_e	91.7	294
	R^2	0.571	0.4997
Pseudo-second order	k_{2p}	3.08×10^{-5}	8.35×10^{-4}
	q_e	278	333
	R^2	$R^2 = 0.5981$	$R^2 = 1$
Intraparticle diffusion	k_{int}	0.0861	6.6788
	R^2	0.9469	0.7128

3.5. Thermodynamics

The values of ΔH and ΔS were determined based on the slope and the intercept from the plot of $\ln(K_d)$ vs. $1/T$ (Figure 12). The values of ΔG were calculated at different temperatures according to Equation (5). The values of ΔH , ΔS and ΔG are presented in Table 4. Corresponding to the results, all values of ΔG are negative for NBB and CV adsorption, indicating that the adsorption process is spontaneous. Further, the values of ΔG (kJ/mol) are in the range of $0 > \Delta G > -20$, suggesting a physical adsorption of both dyes [4]. The positive values of ΔH indicate that the sorption process is endothermic. Moreover, the values of ΔS are positive for both dyes. As a result, ΔG value decreases as the temperature increases. The positive value of ΔS can be attributed to the increase in randomness at the solid–solution interface [17], and this is represented by the following reaction:

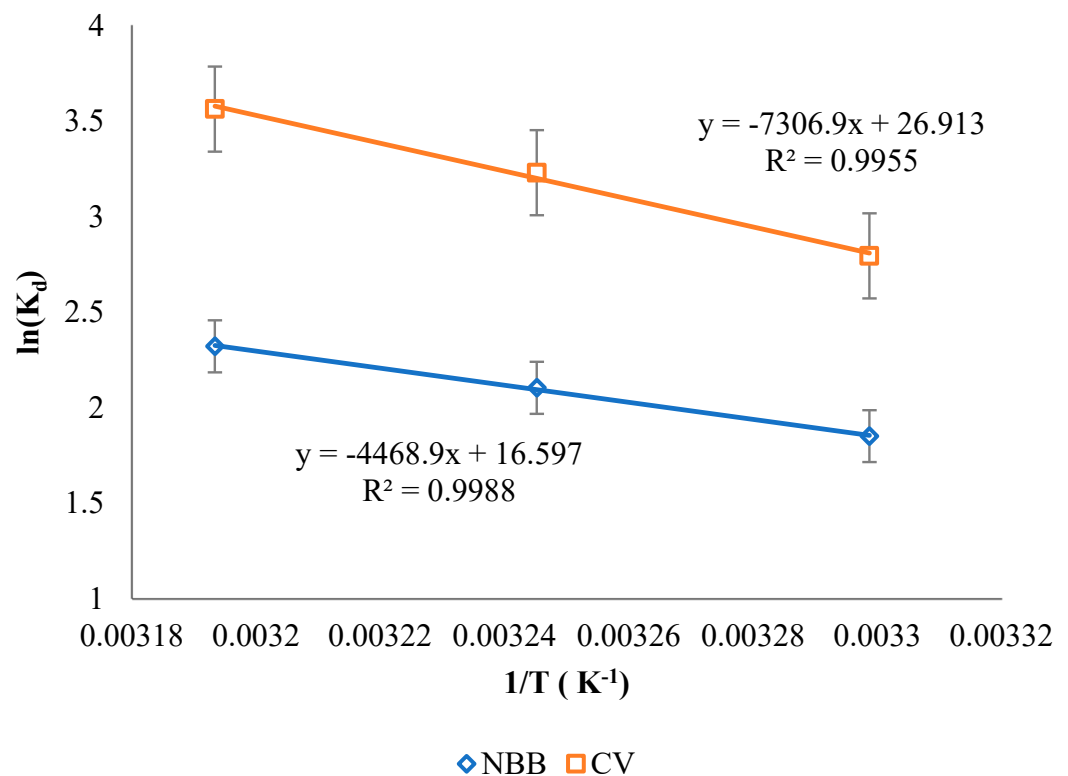


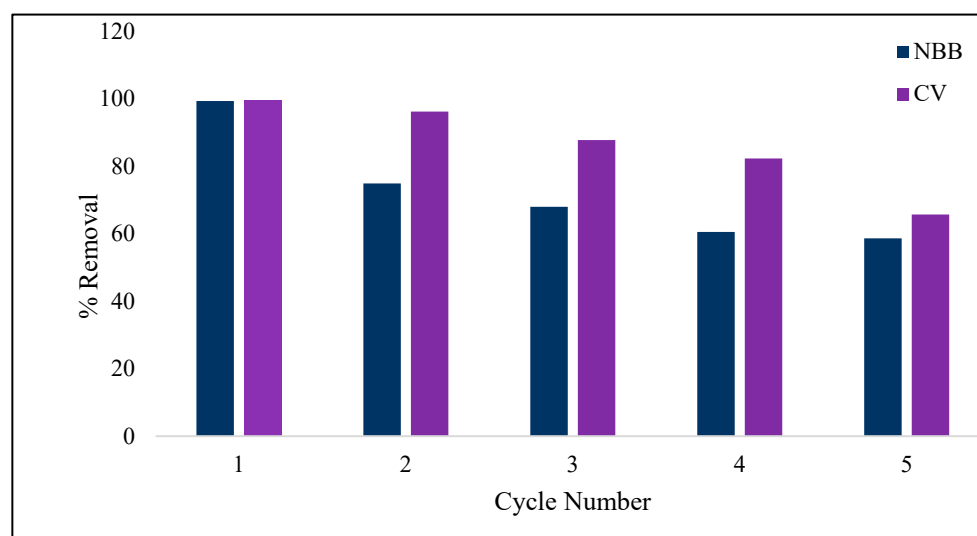
Figure 12. Thermodynamic study for NBB and CV dyes onto ACOC.

Table 4. Thermodynamic parameters for adsorption of NBB and CV on ACOC.

Dye	ΔH (KJ/mol)	ΔS (J/mol)	ΔG (KJ/mol)		
			303 K	308 K	313 K
NBB	37.15	137.99	−4.68	−5.37	−6.06
CV	60.75	223.75	−11.42	−12.61	−13.80

4. Reusability of ACOC

The reusability of ACOC was investigated for five cycles of NBB and CV adsorption. Figure 13 illustrates the recyclability of the adsorbent for five cycles. After five cycles, the adsorption efficiency decreases from 99.4% to 58.7% and from 99.7% to 65.7% for NBB and CV, respectively. The decrease in the adsorption efficiency may be attributed to the loss of ACOC during the washing between cycles, as perhaps not all the aggregated dyes' particles were removed by washing between cycles.

**Figure 13.** Reusability of ACOC for adsorption of NBB and CV.

5. Conclusions

The activated carbon prepared from oak cupules, a cost-free forestry waste, was effectively used to eliminate anionic naphthol blue black dye and the cationic crystal violet dye from an aqueous solution. The findings obtained for NBB and CV adsorption onto ACOC show that the removal efficiency of cationic dye is better than that of anionic dye. The adsorption data were modelled after a Langmuir isotherm model for both dye; the q_m value was found to be 213 and 625 mg g^{-1} for NBB and CV, respectively, and these values indicate high capacity compared to previous studies. The adsorption kinetics of NBB and CV onto ACOC were well fitted using a pseudo-first order model and a pseudo-second order model for NBB and CV, respectively. The adsorption processes of NBB and CV by ACOC were endothermic and spontaneous.

Author Contributions: Conceptualization, M.A. and A.M.A.-M.; methodology, M.A.; formal analysis, G.E., H.A. and T.S.; data curation, G.E., H.A. and T.S.; writing—original draft preparation, M.A.; writing—review and editing, M.A.; project administration, A.M.A.-M. All authors have read and agreed to the published version of the manuscript.

Funding: This research was funded by Isra University with grant number of [8-38/2020/2021].

Institutional Review Board Statement: Not Applicable.

Informed Consent Statement: Not Applicable.

Data Availability Statement: The data are available within the body of the article, and any further data can be requested from authors.

Acknowledgments: All authors greatly appreciate Isra University for funding the project.

Conflicts of Interest: The authors declare that they have no competing interests.

References

1. Visa, M.; Bogatu, C.; Duta, A. Simultaneous Adsorption of Dyes and Heavy Metals from Multicomponent Solutions Using Fly Ash. *Appl. Surf. Sci.* **2010**, *256*, 5486–5491. [[CrossRef](#)]
2. Samchetshabam, G.; Hussan, A.; Choudhury, T. Impact of Textile Dyes Waste on Aquatic Environments and Its Treatment. *Environ. Ecol.* **2016**, *35*, 2349–2353.
3. Berradi, M.; Hsissou, R.; Khudhair, M.; Assouag, M.; Cherkaoui, O.; El Bachiri, A.; El Harfi, A. Textile Finishing Dyes and Their Impact on Aquatic Environ. *Heliyon* **2019**, *5*, e02711. [[CrossRef](#)]
4. Foroutan, R.; Peighambaroust, S.J.; Peighambaroust, S.H.; Pateiro, M.; Lorenzo, J.M. Adsorption of Crystal Violet Dye Using Activated Carbon of Lemon Wood and Activated Carbon/Fe₃O₄ Magnetic Nanocomposite from Aqueous Solutions: A Kinetic, Equilibrium and Thermodynamic Study. *Molecules* **2021**, *26*, 2241. [[CrossRef](#)]
5. Đorđević, J.S.; Vladislavljević, G.T.; Trtić-Petrović, T.M. Removal of the Selected Pesticides from a Water Solution by Applying Hollow Fiber Liquid–Liquid Membrane Extraction. *Ind. Eng. Chem. Res.* **2014**, *53*, 4861–4870. [[CrossRef](#)]
6. Bakry, A.M.; Alamier, W.M.; Salama, R.S.; Samy El-Shall, M.; Awad, F.S. Remediation of Water Containing Phosphate Using Ceria Nanoparticles Decorated Partially Reduced Graphene Oxide (CeO₂-PRGO) Composite. *Surf. Interfaces* **2022**, *31*, 102006. [[CrossRef](#)]
7. Mansour, R.A.E.-G.; Sameda, M.G.; Zaatout, A.A. Removal of Brilliant Green Dye from Synthetic Wastewater under Batch Mode Using Chemically Activated Date Pit Carbon. *RSC Adv.* **2021**, *11*, 7851–7861. [[CrossRef](#)] [[PubMed](#)]
8. Sharma, G.; Sharma, S.; Kumar, A.; Lai, C.W.; Naushad, M.; Shehnaz; Iqbal, J.; Stadler, F.J. Activated Carbon as Superadsorbent and Sustainable Material for Diverse Applications. *Adsorpt. Sci. Technol.* **2022**, *2022*, e4184809. [[CrossRef](#)]
9. Haji, A.; Mahmoodi, N.M. Soy Meal Hull Activated Carbon: Preparation, Characterization and Dye Adsorption Properties. *Desalination Water Treat.* **2012**, *44*, 237–244. [[CrossRef](#)]
10. Boudechiche, N.; Fares, M.; Ouyahia, S.; Yazid, H.; Trari, M.; Sadaoui, Z. Comparative Study on Removal of Two Basic Dyes in Aqueous Medium by Adsorption Using Activated Carbon from Ziziphus Lotus Stones. *Microchem. J.* **2019**, *146*, 1010–1018. [[CrossRef](#)]
11. Bhowmik, S.; Chakraborty, V.; Das, P. Batch Adsorption of Indigo Carmine on Activated Carbon Prepared from Sawdust: A Comparative Study and Optimization of Operating Conditions Using Response Surface Methodology. *Results Surf. Interfaces* **2021**, *3*, 100011. [[CrossRef](#)]
12. Seidmohammadi, A.; Asgari, G.; Dargahi, A.; Leili, M.; Vaziri, Y.; Hayati, B.; Shekarchi, A.A.; Mobarakian, A.; Bagheri, A.; Nazari, et al. A Comparative Study for the Removal of Methylene Blue Dye from Aqueous Solution by Novel Activated Carbon Based Adsorbents. *Prog. Color Color. Coat.* **2019**, *12*, 133–144. [[CrossRef](#)]
13. Djilani, C.; Zaghoudi, R.; Djazi, F.; Bouchekima, B.; Lallam, A.; Modarressi, A.; Rogalski, M. Adsorption of Dyes on Activated Carbon Prepared from Apricot Stones and Commercial Activated Carbon. *J. Taiwan Inst. Chem. Eng.* **2015**, *53*, 112–121. [[CrossRef](#)]
14. Astuti, F.; Sari, N.; Maghfirohtuzzoimah, V.L.; Asih, R.; Baqiya, M.A.; Darminto, D. Study of the Formation of Amorphous Carbon and RGO-like Phases from Palmyra Sugar by Variation of Calcination Temperature. *J. Fis. Dan Apl.* **2020**, *16*, 91. [[CrossRef](#)]
15. Aljeboree, A.M.; Alshirifi, A.N.; Alkaim, A.F. Kinetics and Equilibrium Study for the Adsorption of Textile Dyes on Coconut Shell Activated Carbon. *Arab. J. Chem.* **2017**, *10*, S3381–S3393. [[CrossRef](#)]
16. Litefti, K.; Freire, M.S.; Stitou, M.; González-Álvarez, J. Adsorption of an Anionic Dye (Congo Red) from Aqueous Solutions by Pine Bark. *Sci. Rep.* **2019**, *9*, 16530. [[CrossRef](#)] [[PubMed](#)]
17. Saha, P.; Chowdhury, S. Insight into Adsorption Thermodynamics. *Thermodynamics* **2011**, *16*, 349–364. [[CrossRef](#)]

Disclaimer/Publisher’s Note: The statements, opinions and data contained in all publications are solely those of the individual author(s) and contributor(s) and not of MDPI and/or the editor(s). MDPI and/or the editor(s) disclaim responsibility for any injury to people or property resulting from any ideas, methods, instructions or products referred to in the content.